

Ferrimagnetism and defect clusters in Fe_{1-x}O films

D. V. Dimitrov, K. Unruh, and G. C. Hadjipanayis

Department of Physics and Astronomy, University of Delaware, Newark, Delaware 19716

V. Papaefthymiou

Department of Physics, University of Ioannina, 451 10 Ioannina, Greece

A. Simopoulos

NCSR Demokritos, 15310 Aghia Paraskevi, Attikis, Athens, Greece

(Received 27 July 1998; revised manuscript received 26 October 1998)

Nonstoichiometric single phase Fe_{1-x}O films with ferrimagnetic properties, large saturation magnetization (M_s), and low-temperature coercivity (H_c) have been prepared and studied. A model on the relation between M_s and the lattice parameter (a) is proposed. The model is based on the existence of 16:5 spinel-type defect clusters, and predicts a linear dependence between M_s and a . The experimental data of M_s versus a is a straight line passing through the point (M_s, a) of bulk Fe_3O_4 . This fact suggests that Fe_{1-x}O is the link between the two phases Fe_3O_4 and FeO , which have seemingly different physical nature and properties, into one class of materials. [S0163-1829(99)08221-1]

INTRODUCTION

The iron oxide system is very rich and complicated and comprised of a number of phases with different stoichiometry, crystal structures, magnetic and electronic behavior, and phase transitions. Different iron oxides have been intensively studied and a large number of exciting phenomena have been discovered, including, the anomalous moment and anisotropy behavior in Fe_3O_4 films,² the observation of interfacial electrical polarization in $\text{Fe}_3\text{O}_4/\text{NiO}$ superlattices,³ spin canting and finite-size effects in $\gamma\text{-Fe}_2\text{O}_3$ particles,⁴ spin-glass ordering in $\gamma\text{-Fe}_2\text{O}_3$ particles,⁵ observation of charge freezing at room temperature in (100) magnetite,⁶ and a number of others, which cannot be mentioned here due to space limitations. In addition, there have been a vast number of studies on optimizing the microstructure of magnetic recording materials based on $\gamma\text{-Fe}_2\text{O}_3$ and mixtures of $\gamma\text{-Fe}_2\text{O}_3$ with Fe_3O_4 .

Fe_3O_4 has the inverse spinel crystal structure, where eight Fe^{3+} ions occupy tetrahedrally coordinated interstitial sites (A), and another eight Fe^{3+} plus eight Fe^{2+} ions occupy 16 of the octahedrally coordinated interstitial sites (B) in the close-packed face-centered cubic (fcc) O^{2-} lattice. One of the most interesting phenomena in Fe_3O_4 is the charge ordering and the corresponding phase transition (Verwey transition), which for bulk samples occurs at 123 K. For decades this effect has attracted enormous interest (for review and references see Ref. 7) and is still not understood. Fe_3O_4 is a ferrimagnet, with antiparallel A and B sublattice magnetizations, which is a result of the superexchange interactions through the p orbitals of O^{2-} ions.

Even though it attracted significantly less interest than the Fe_3O_4 , $\gamma\text{-Fe}_2\text{O}_3$ and $\alpha\text{-Fe}_2\text{O}_3$ phases, the FeO phase is very interesting on its own. Stoichiometric FeO is antiferromagnetic (AF) with a rocksalt crystal structure, best described as a close-packed fcc O^{2-} lattice with Fe^{2+} ions on all B interstitial sites. FeO is almost universally nonstoichiometric with

some Fe deficiency and is denoted as Fe_{1-x}O . It has interesting electronic properties; it is an intrinsic semiconductor with a p - n transition at x around 0.08.⁸ Neutron-diffraction⁹ and x-ray-scattering¹⁰ studies on Fe_{1-x}O quenched powders and single crystals indicated that the vacancies were not randomly distributed but clustered around Fe^{3+} ions located on A sites. Significant progress toward understanding the possible structure of defect clusters was achieved in the theoretical work of Catlow and Fender.¹

The initial studies on Fe_{1-x}O suggested an AF order with a corresponding low magnetic moment. Recently anomalously high magnetization was found in sputtered Fe_{1-x}O films.^{11,12} Even though it was speculated that the origin of the large magnetic moment is due to defect clusters, no specific mechanism and details were offered. The present work shows how the magnetic behavior is related to the presence of large agglomerates of 16:5 defect clusters, originally proposed in Ref. 1. A phenomenological model on the saturation magnetization (M_s) versus the lattice parameter (a) is proposed and compared against our experimental data. The results of this analysis showed that there is a fundamental relationship between Fe_{1-x}O and Fe_3O_4 , indications of which were found long time ago in the lattice parameter versus vacancy concentration¹³ and the heats of formation studies.¹⁴

DEFECT CLUSTERS IN Fe_{1-x}O

The work of Catlow and Fender had a detailed and complete analysis on the different type of defect clusters in Fe_{1-x}O including the energetics of their formation. Nevertheless, for clarity and convenience, it is useful to include a brief discussion on the major defect clusters and their features. For more details the reader can see the original works.^{1,10}

By taking one Fe^{2+} ion out of the FeO crystal a vacancy is created. Correspondingly, two of the original Fe^{2+} ions should give away an additional electron and become Fe^{3+} in

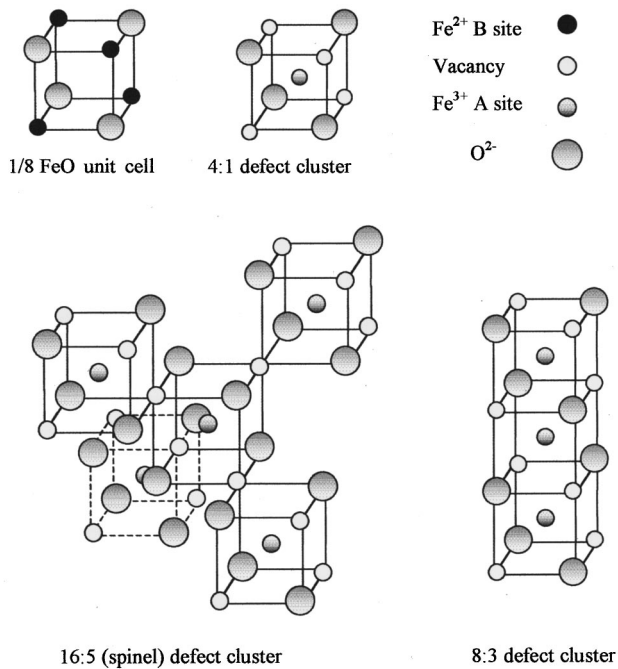


FIG. 1. Schematics of one eighth of the FeO unit cell, 4:1, 16:5, and 8:3 defect clusters.

order to ensure overall electroneutrality. The vacancy has a negative charge, so one can think that two of the neighboring octahedral Fe ions will become triply ionized to compensate for the negative charge. The Coulomb interaction between a vacancy and two neighboring Fe³⁺ on B sites creates large electrostatic energy. This energy can be substantially reduced by moving one of the Fe³⁺ ions to an A site and surrounding it with four vacancies, creating the so-called 4:1 defect cluster. The first number states the number of vacancies and the second the number of Fe³⁺ ions on A sites per cluster. The 4:1 cluster proved to be a major building block for further agglomeration and defect cluster growth occurring in two major ways, by corner or by edge sharing. The largest binding energy per vacancy (2.52 eV) was found in the edge sharing 8:3 cluster. However, the 16:5 corner-sharing cluster had the highest symmetry and second highest binding energy (2.38 eV). The 13:4 cluster originally proposed by Koch and Cohen has a lower binding energy (2.10 eV). Because of this Catlow and Fender argued that it does not occur frequently.¹ The initial building block, which is essentially (1/8) of the FeO unit cell, plus the 4:1, 8:3, and 16:5 clusters, is shown in Fig. 1. In the 16:5 cluster, each vacancy is shared by no more than two A Fe³⁺, and it is essentially an element of the inverse spinel structure of Fe₃O₄.

If further cluster growth is to occur, it is important to question which way is energetically more favorable, to stack 8:3 or 16:5 defect clusters? The calculations of Catlow and Fender showed that for further growth one expects agglomeration of 16:5 clusters to be, by far, more favorable. One does not need elaborate crystal energy calculations to figure out the reason for this. The cluster has a large negative charge ($7e^-$ for 8:3 and $17e^-$ for 16:5), which should be screened fast by surrounding the cluster with Fe³⁺ on B sites. Looking at Fig. 1 one sees that this can be done by Fe³⁺ on

B sites in between the 4:1 building blocks and it is possible to attach two, or if needed more, 16:5 clusters on their corners without increasing the electrostatic energy. In contrast the 8:3 cluster is compact and the screening should come from Fe³⁺ ions surrounding the cluster. This fact prohibits further cluster growth, because the electrostatic energy increases very fast. Catlow argued that large 16:5 clusters can exist at low temperatures. However, at high temperatures they will break up into small 4:1 and 8:3 clusters to provide an increase in the entropy. A similar situation should exist in quenched samples, which are snapshots of the high-temperature equilibrium state.

EXPERIMENTAL PROCEDURES

Fe_{1-x}O films, about 3500 Å thick, have been prepared by reactive dc magnetron sputtering in a O₂/Ar mixture on water-cooled Kapton and glass substrates. Details about the deposition conditions, thickness determination, microstructural, and Mössbauer characterization were given previously.^{15,16}

The x-ray-diffraction spectra were collected by a θ - 2θ powder diffractometer equipped with a θ compensating slit. The peak positions were determined by fitting the peak with a Pearson VII function¹⁷ using the PEAKFIT program from Jandel Scientific. The systematic errors of the x-ray diffractometer were determined using the following procedure. The spectrum of a quartz (SiO₂) standard was collected 10 times and the average peak positions were calculated. The position of the peaks were very reproducible, and the difference between an arbitrary peak and its average was never larger than 0.02°. The theoretical SiO₂ peak positions were calculated by using their d spacings¹⁸ and Bragg's law;

$$2d_{hkl} \sin(\theta) = \lambda, \quad (1)$$

where d_{hkl} was the d spacing for an (hkl) Bragg reflection and the x-ray wavelength was $\lambda = 1.54056 \text{ \AA}$ (Cu $K\alpha 1$). Having determined the experimental and theoretical positions of the SiO₂ standard, a curve of the systematic errors of the diffractometer as a function of the angle was created. This curve has been used to correct the positions of the measured peaks. The procedure was tested on a number of materials with well-known lattice parameters and crystal structures, including α -Al₂O₃, α -Fe₂O₃, and TiO₂. The error of the d -spacing determination in all cases was less than 0.1%. The same procedure was used to determine the d spacings of the Fe_{1-x}O films. For all the films, whose data will be discussed, the x-ray-diffraction data showed the presence of only FeO peaks. Some of the films were checked with Mössbauer spectroscopy, which confirmed the conclusion that the films were comprised of single phase Fe_{1-x}O.

Magnetic data were collected using superconducting quantum interference device magnetometry between 10 and 380 K with 5.5 T maximum applied field.

MAGNETIC PROPERTIES OF Fe_{1-x}O FILMS

The magnetization measurements of reactively sputtered Fe_{1-x}O films surprisingly revealed hysteresis loops with large saturation magnetization (M_s) and low-temperature coercivity (H_c). In the present work the properties of five

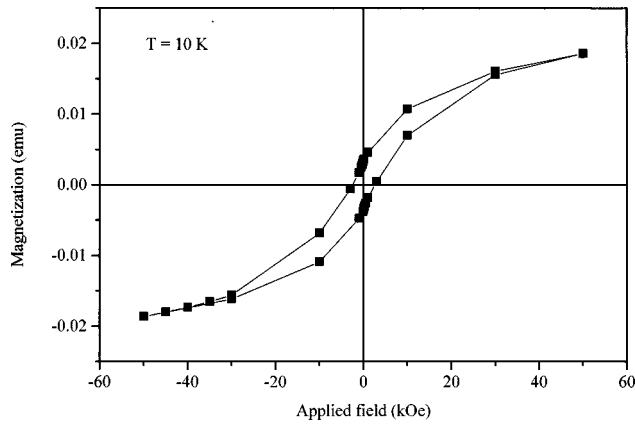


FIG. 2. Low-temperature hysteresis loop of a typical off-stoichiometric $Fe_{1-x}O$ film.

$Fe_{1-x}O$ films, with lattice parameter (a) varying between 4.256 and 4.294 Å, will be discussed. In addition, magnetic data on commercial bulk $Fe_{1-x}O$ powder ($a=4.303$ Å) from Cerac Inc. will be included. A low-temperature hysteresis loop of a typical $Fe_{1-x}O$ sample ($a=4.275$ Å) is shown in Fig. 2. Figure 3(a) shows the temperature dependence of H_c and Fig. 3(b) shows a typical low-field magnetization versus a temperature curve. M_s in some samples was as high as 275 emu/cc ($a=4.256$ Å) and H_c at 10 K about 3 kOe for all of the films. These data are very unusual and interesting because for a long time $Fe_{1-x}O$ has been considered to be AF with a weak magnetic response. Magnetic data on $Fe_{1-x}O$ powders quenched from high temperature⁹ had a weak magnetic response, which was explained assuming AF order. As

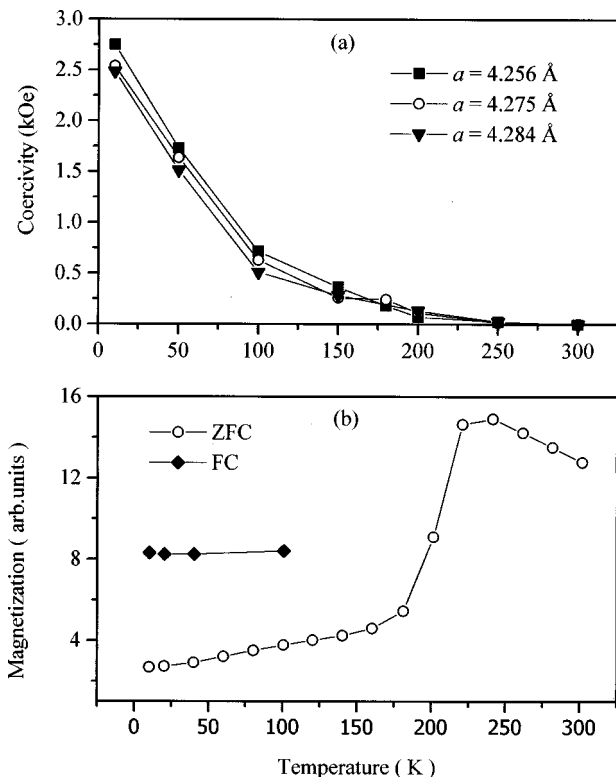


FIG. 3. Temperature dependence of H_c (top) and low-field magnetization versus temperature data (bottom) of a few representative samples.

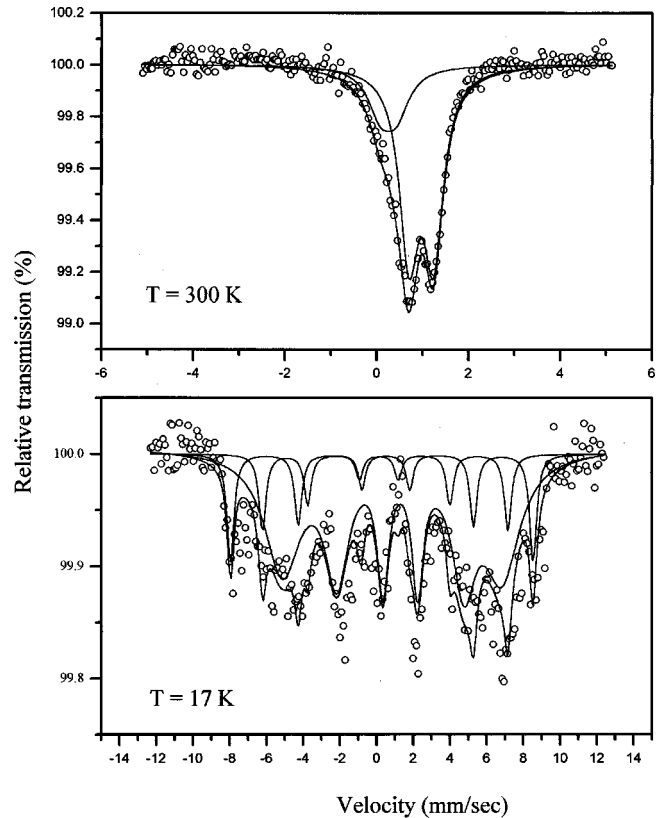


FIG. 4. Low- and room-temperature Mössbauer spectra of a representative $Fe_{1-x}O$ film.

we have implied earlier, the difference between our films and the quenched powders is most probably due to the size of the defect cluster. At high temperatures small clusters are predominantly found and fast quenching preserves them at low temperatures. The net moment on these small clusters is negligible and is not observed. However, a very different situation occurs in reactively sputtered films. It seems that deposition on a cold substrate favors the growth of large defect clusters which, as we have discussed earlier, should be aggregates of spinel 16:5 building blocks.

The coercivity decreases fast with temperature and becomes negligible above 200 K for all $Fe_{1-x}O$ films [Fig. 3(a)]. The temperature where H_c disappears is practically the Néel temperature of FeO ($T_N=198$ K). In addition, there is a corresponding steep increase in the zero-field-cooled magnetization of the M vs T data, which indicates the large influence of the AF matrix on magnetic properties. These features will be discussed in detail, after we present a phenomenological model on the origin of the magnetization in these films. For the time being, the fact that H_c becomes negligible above 200 K suggests that the sample is superparamagnetic. This effect alone is not an unambiguous proof for superparamagnetism and further tests are usually needed. In our work the proof was provided by Mössbauer studies. Low-temperature ($T=17$ K) Mössbauer spectra were magnetically split indicating a significant hyperfine field (H_{hf}) and an AF magnetic order (Fig. 4), while the RT (300 K) spectrum was a doublet, characteristic of a zero hyperfine field and superparamagnetism.

Knowing that the sample is in the superparamagnetic state, allows one to determine the average magnetic moment

per defect cluster (μ) and consequently its volume. For that purpose measurements of the magnetization curve at temperatures above the blocking temperature (T_B) are used. If the distribution function of the defect cluster volumes in the sample is $f(V)$, one can write down the following equation for M as a function of the applied magnetic field H :

$$M = M_s \int_0^\infty L\left(\frac{M_s V H}{k_B T}\right) f(V) dV, \quad (2)$$

where L denotes the Langevin function,

$$L(x) = \coth(x) - \frac{1}{x}. \quad (3)$$

Fitting the magnetization curve to Eq. (2) without a reliable distribution function $f(V)$ can be a difficult and error prone procedure. However, to determine M_s and μ there is no need to know the exact form of $f(V)$. To find M_s one can use the high-field region (H larger than 10 kOe) where $\coth(M_s V H / k_B T)$ is practically 1. This allows one to write

$$M = M_s \int_0^\infty \left(1 - \frac{k_B T}{M_s V H}\right) f(V) dV. \quad (4)$$

Finally working out the integral one obtains that M is a linear function of H^{-1} and the intercept at the $H^{-1} = 0$ axis is M_s ,

$$M = M_s - k_B T \langle (V^{-1}) \rangle H^{-1}. \quad (5)$$

Using the value of M_s , one can estimate the average magnetic moment per cluster (μ) by using low-field magnetization data. For small x (small H) the Langevin function $L(x)$ is approximated by $x/3$, and the normalized magnetization (m) can be written as

$$m = \frac{M}{M_s} = \int_0^\infty \frac{M_s V H}{3 k_B T} f(V) dV = \frac{\mu H}{3 k_B T}. \quad (6)$$

The value of μ can be determined by taking the derivative of m with respect to H and evaluating it at $H = 0$

$$\mu = 3 k_B T \left(\frac{dm}{dH} \right)_{H=0}. \quad (7)$$

The average magnetic moment per cluster was determined using the described method, and was found to be between 5000 and 5500 μ_B with one exception where it was significantly larger (9000 μ_B). No correlation between μ and M_s or a was found. The important point is that the defect cluster is three orders of magnitude larger than the cluster size considered by Catlow and Fender. We have already discussed that large clusters can only be built by aggregating 16:5 spinel clusters which share common corners. This conclusion is used as a basis for the next section where a functional dependence between M_s and a is proposed.

THE RELATIONSHIP BETWEEN M_s AND a IN NONSTOICHIOMETRIC Fe_{1-x}O

There have been a number of studies on the relation between the lattice parameter (a) of bulk Fe_{1-x}O and its off-

stoichiometry value (x), which was commonly found to be a linear function

$$\alpha = A[1 - Bx], \text{ or } x = C[D - a]. \quad (8)$$

The data of a number of studies were summarized in Ref. 19 and the values for the average parameters were $A = 4.333 \text{ \AA}$, $B = 0.0979 \text{ \AA}$, $C = 2.358 \text{ \AA}$, $D = 4.333 \text{ \AA}$. If one denotes the number of Fe^{3+} by y , and keeps in mind that the oxygen ions always get two electrons to saturate their valence (O^{2-}), one can write the equation for charge conservation. When the equation is solved for y one finds

$$y = 2x. \quad (9)$$

In nonstoichiometric Fe_{1-x}O the number of Fe^{3+} ions is always $2x$ and the number of Fe^{2+} is $(1 - 3x)$. This result is universal for all iron oxides, and is easily verifiable for Fe_3O_4 and the two different Fe_2O_3 oxides.

The defect clusters in our films are large agglomerates of 16:5 spinel building blocks, which allow us to think of an Fe_{1-x}O film as comprised of an Fe_3O_4 -like phase coherently embedded in an ideal FeO matrix. The $2x$ Fe^{3+} ions need x Fe^{2+} ions and $4x$ O^{2-} ions to form x molecules of Fe_3O_4 . After the formation of x Fe_3O_4 molecules, there are $(1 - 4x)$ Fe^{2+} and $(1 - 4x)$ O^{2-} ions left, which match exactly to form $(1 - 4x)$ molecules of an ideal FeO matrix. Neglecting the small difference between the lattice parameters (3%) of the close-packed fcc oxygen lattice in FeO and Fe_3O_4 , one can conclude that the volume fraction of the defect clusters is $4x$ and the rest $(1 - 4x)$ belongs to the perfect FeO phase. The FeO matrix is antiferromagnetic and contributes a negligible magnetic signal in the relatively small fields used to measure the magnetization of the samples. The observed magnetization comes exclusively from the Fe_3O_4 defect clusters. It is natural to assume that the saturation magnetization of the defect clusters is the same as that of the Fe_3O_4 phase, which allows one to write the total saturation magnetization of the Fe_{1-x}O film as

$$M_s(\text{Fe}_{1-x}\text{O}) = 4x M_s(\text{Fe}_3\text{O}_4). \quad (10)$$

$M_s(\text{Fe}_{1-x}\text{O})$ is the saturation magnetization of Fe_{1-x}O films and $M_s(\text{Fe}_3\text{O}_4)$ is the saturation magnetization of Fe_3O_4 phase (510 emu/cc at 10 K and 480 emu/cc at 300 K).

Using the linear dependence of x on a [Eq. (8)] one finds that M_s should also depend on x linearly:

$$M_s(\text{Fe}_{1-x}\text{O}) = \{4C M_s(\text{Fe}_3\text{O}_4)\} [D - a]. \quad (11)$$

Figure 5 is a plot of the experimental M_s versus a data and the least-squares linear fit through it ($C = 2.07$ and $D = 4.318 \text{ \AA}$). For comparison, a M_s vs a straight line was generated by using the C and D values derived from the data in Ref. 19 as shown in Fig. 5. It predicts a considerably larger M_s than our data. However, the straight line from the fit of our data passes through the M_s of Fe_3O_4 , which is to be expected from our model. After all, in the spirit of our analysis, Fe_3O_4 can be considered as nonstoichiometric $\text{Fe}_{(1-0.25)}\text{O}$ in which the whole FeO matrix has been transformed into a giant spinel defect cluster.

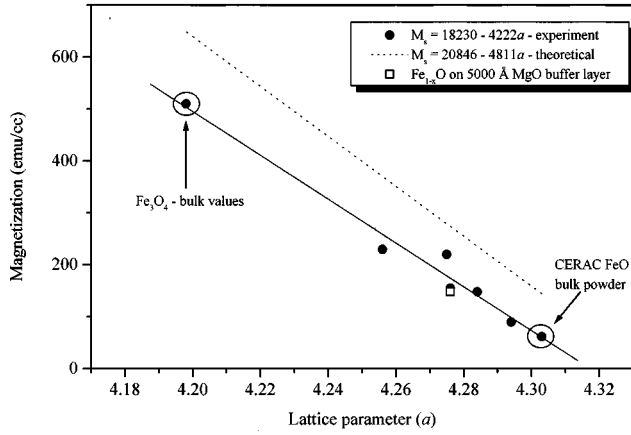


FIG. 5. Saturation magnetization versus lattice parameter. Data fit well to a linear function passing through the bulk Fe_3O_4 values.

We believe that our M_s vs a data indicate the existence of a fundamental relationship between FeO and Fe_3O_4 and that the nonstoichiometric Fe_{1-x}O is the bridge between them.

COERCIVITY IN Fe_{1-x}O FILMS

In this last section the origin of the large H_c at low temperature in Fe_{1-x}O films is discussed. As shown before the films were superparamagnetic at room temperature and their magnetization curve was used to estimate the average magnetic moment. Before the analysis of H_c and its temperature dependence is done, it is necessary to clarify the microstructure of the samples. Transmission electron microscopy (TEM) and x-ray diffraction (Scherrer formula) indicated that the films were polycrystalline with a columnar microstructure.²⁰ The base was oval with a typical diameter of about 10 nm while the height varied between 50 and 80 nm. It is natural to consider that each defect cluster is located in an individual grain and does not spread over two or more grains. Because the area where two cylinders touch is small, the exchange coupling between two grains is negligible. However, the exchange interactions between the defect cluster and the antiferromagnetic part of the rest of the grain are large and affect the magnetic properties substantially. As a result of the strong coupling, the magnetic moment of the defect cluster and the two AF sublattice magnetizations rotate simultaneously when the field approaches large negative values. The rotation is against the anisotropy energy of the AF part of the grain but is assisted by thermal activation at higher temperatures. This analysis is strongly supported by the temperature dependence of H_c to follow.

For temperatures below T_B , the H_c of an ensemble of superparamagnetic grains is different from zero and its temperature dependence is usually described by

$$H_c = H_c(0) \left(1 - \sqrt{\frac{T}{T_B}} \right). \quad (12)$$

The H_c vs T data below T_B and its fit against [Eq. (12)] of a typical sample ($a = 4.264 \text{ \AA}$) are shown in Fig. 6. For this particular sample $H_c(0)$ was 3180 Oe and T_B was 196 K, which is essentially the same as the $T_N = 198 \text{ K}$. The differ-

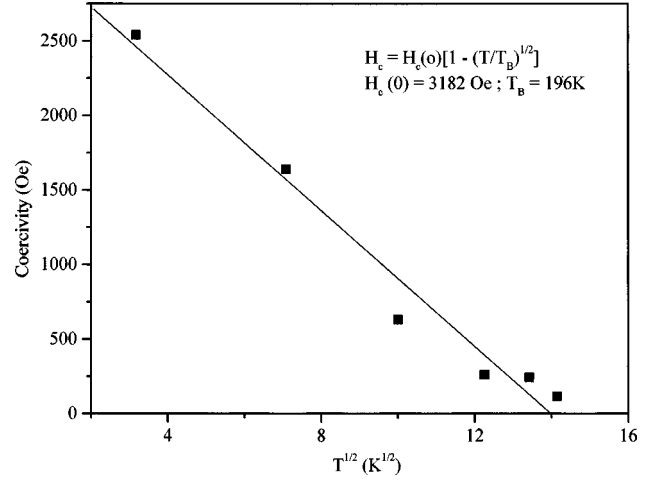


FIG. 6. Fit of the H_c data of a representative Fe_{1-x}O film against Eq. (12).

ence between T_N and T_B was less than 10 K in all films. The blocking temperature of the defect cluster can also be estimated by using

$$25k_B T_B = KV, \quad (13)$$

where K is the anisotropy constant and V is the volume of the grain (defect cluster). The volume of a cluster with a magnetic moment of $5300\mu_B$ is $2.88 \times 10^{-19} \text{ cm}^3$. Using the value of the magnetocrystalline anisotropy of Fe_3O_4 ($K = 1.1 \times 10^5 \text{ ergs/cm}^3$) we estimate $T_B \cong 10 \text{ K}$. If the defect clusters were isolated, H_c should be zero for temperatures as low as 10 K. However, as we argued previously, the defect clusters are coupled to the antiferromagnetic FeO part of the grain with the strong superexchange through the p orbitals of O^{2-} . The exchange interactions with the AF FeO matrix oppose the torque from the external magnetic field (H). In order for the magnetization reversal to occur, the external magnetic field should overcome the magnetocrystalline anisotropy energy of the AF FeO grain, so that the defect cluster magnetization and the FeO sublattice magnetizations rotate and switch in unison. As a result of this argument the low-temperature H_c can be defined by the equation (V_{AF} is the volume of the AF grain and V_{dc} the volume of the defect cluster):

$$2M_s(\text{Fe}_3\text{O}_4)V_{\text{dc}}H_c = K_{\text{AF}}V_{\text{AF}}. \quad (14)$$

To the best of our knowledge we do not know a good estimate of the magnetocrystalline anisotropy coefficient in small grains of FeO. However, an order of magnitude estimate can be done by using the fact that the anisotropy of AF oxides is of the same order but smaller than that of the corresponding ferrimagnetic oxides. Using $K_{\text{AF}} = 6 \times 10^4 \text{ ergs/cm}^3$ and $V_{\text{dc}} \cong V_{\text{AF}}$ (estimated from the M_s of this sample) leads to $H_c \cong 2900 \text{ Oe}$ in qualitative agreement with the experimental value. When the temperature is increased, thermal fluctuations assist the external magnetic field to overcome the anisotropy energy barrier and lead to the observed fast H_c decrease, which agrees well with the theoretical prediction for superparamagnetic particles [Eq. (12)]. Other evidence for the strong influence of the AF FeO matrix

on the magnetization reversal, in particular the large unidirectional anisotropy and shifted hysteresis loops in field-cooled samples, has been discussed in our previous works.¹⁶

In summary, ferrimagnetism was observed in reactively sputtered nonstoichiometric Fe_{1-x}O films. A model based on the existence of large agglomerations of 16:5 defect clusters predicts a linear dependence between M_s and a , which was

experimentally observed. The coercive field is entirely dominated by the exchange interactions with the AF FeO matrix.

ACKNOWLEDGMENTS

This work was supported by NSF Grant No. DMR 9307676.

-
- ¹C. R. A. Catlow and B. E. F. Fender, *J. Phys. C* **8**, 3267 (1975).
²D. T. Margulies, F. T. Parker, F. E. Spada, R. S. Goldman, J. Li, R. Sinclair, and A. E. Berkowitz, *Phys. Rev. B* **53**, 9175 (1996).
³G. Chern, S. D. Berry, H. Mathias, and L. R. Testardi, *Phys. Rev. Lett.* **68**, 114 (1992).
⁴F. T. Parker, M. W. Foster, D. T. Margulies, and A. E. Berkowitz, *Phys. Rev. B* **47**, 7885 (1993).
⁵S. Mørup, F. Bødker, P. V. Hendriksen, and S. Linderorth, *Phys. Rev. B* **52**, 287 (1995).
⁶J. M. D. Coey and I. V. Shvets, *J. Appl. Phys.* **73**, 6742 (1993).
⁷*Philos. Mag. B* **42**, 1 (1980), entire issue dedicated to the Verwey transition.
⁸D. P. Johnson, *Solid State Commun.* **7**, 1785 (1969).
⁹W. L. Roth, *Acta Crystallogr.* **13**, 140 (1960).
¹⁰F. Koch and J. B. Cohen, *Acta Crystallogr., Sect. B: Struct. Crystallogr. Cryst. Chem.* **25**, 275 (1969).
¹¹Y. K. Kim and M. Oliveria, *J. Appl. Phys.* **75**, 431 (1994).
¹²D. V. Dimitrov, G. C. Hadjipanayis, V. Papaefthymiou, and A. Simopoulos, *IEEE Trans. Magn.* **33**, 4363 (1997).
¹³E. R. Jette and F. Foote, *J. Chem. Phys.* **1**, 29 (1933).
¹⁴L. S. Darken and R. W. Curry, *J. Am. Chem. Soc.* **67**, 1398 (1945).
¹⁵D. V. Dimitrov, G. C. Hadjipanayis, V. Papaefthymiou, and A. Simopoulos, *J. Vac. Sci. Technol. A* **15**, 1473 (1997).
¹⁶D. V. Dimitrov, G. C. Hadjipanayis, V. Papaefthymiou, A. Simopoulos, and C. P. Swann, *IEEE Trans. Magn.* **33**, 4363 (1997).
¹⁷M. M. Hall, Sr., V. G. Veeraraqhavan, H. Rubin, and P. G. Winchell, *J. Appl. Crystallogr.* **10**, 66 (1977).
¹⁸*Natl. Stand. Ref. Data Ser. (U.S. Natl. Bur. Stand.)* **25**, 18 (1981).
¹⁹*Fe Oxides and Fe-Me-O Compounds*, Landolt-Börnstein, New Series, Group III, Vol. 4a (Springer-Verlag, Berlin, 1970), Chap. 1.
²⁰D. V. Dimitrov, Ph.D. thesis, University of Delaware, 1998.